Electronic Supplementary Material (ESI) for Physical Chemistry Chemical Physics.

Supporting Information

Performance Limitations in Thieno[3,4-c]pyrrole-4,6-dione-based Polymers:ITIC Solar Cells

Fan Yang,[†] Deping Qian,[‡] Ahmed Hesham Balawi,[§] Yang Wu,[⊥] Wei Ma,[⊥] Frédéric Laquai,*[,§] Zheng Tang,*[,‖] Fengling Zhang*[,‡] and Weiwei Li*[,†]

[†] Beijing National Laboratory for Molecular Sciences, Key Laboratory of Organic Solids, Institute of Chemistry, Chinese Academy of Sciences, Beijing 100190, PR China

[‡] Biomolecular and Organic Electronics, Department of Physics, Chemistry and Biology, Linköping University, SE-581 83, Linköping, Sweden

[§] King Abdullah University of Science and Technology (KAUST), KAUST Solar Center (KSC), Physical Sciences and Engineering Division (PSE), Material Science and Engineering Program (MSE), Thuwal 23955-6900, Kingdom of Saudi Arabia

[⊥] State Key Laboratory for Mechanical Behavior of Materials, Xi'an Jiaotong University, Xi'an 710049, P. R. China

[‖] Institut für Angewandte Photophysik, Technische Universität Dresden, George-Bähr-Straße 1, 01069, Dresden,Germany

Contents

1. Materials and measurements

The electron acceptor ITIC were purchased from Solarmer Materials Inc. The polymers PTPD3T[S1] , PTPD2T[S2] and PTPDBDT[S3] were synthesized according to literature procedures. Molecular weight was determined with GPC at 140 °C on a PL-GPC 220 system using a PL-GEL 10 μm MIXED-B column and *o*-DCB as the eluent against polystyrene standards. Low concentration of 0.1 mg mL^{-1} polymer in *o*-DCB was applied to reduce aggregation. Optical absorption spectra were recorded on a JASCO V-570 spectrometer with a slit width of 2.0 nm and a scan speed of 1000 nm min^{-1}. Cyclic voltammetry was performed under an inert atmosphere at a scan rate of 0.1 V s^{-1} and 1 M tetrabutylammonium hexafluorophosphate in acetonitrile as the electrolyte, a glassy-carbon working electrode coated with samples, a platinum-wire auxiliary electrode, and an Ag/AgCl as a reference electrode. Atomic force microscopy (AFM) images were recorded using a Digital Instruments Nanoscope IIIa multimode atomic force microscope in tapping mode under ambient conditions.

GIWAXS measurements were performed at beamline 7.3.3[S4] at the Advanced Light Source. Samples were prepared on Si substrates using identical blend solutions as those used in devices. The 10 keV X-ray beam was incident at a grazing angle of 0.12°-0.16°, selected to maximize the scattering intensity from the samples. The scattered x-rays were detected using a Dectris Pilatus 2M photon counting detector. R-SoXS transmission measurements were performed at beamline 11.0.1.2[S5] at the Advanced Light Source (ALS). Samples for R-SoXS measurements were prepared on a PEDOT:PSS modified Si substrate under the same conditions as those used for device fabrication, and then transferred by floating in water to a 1.5 mm × 1.5 mm, 100 nm thick Si3N4 membrane supported by a 5 mm × 5 mm, 200 μm thick Si frame (Norcada Inc.). 2-D scattering patterns were collected on an in-vacuum CCD camera (Princeton Instrument PI-MTE). The sample detector distance was calibrated from diffraction peaks of a triblock copolymer poly(isoprene-*b*-styrene-*b*-2-vinyl pyridine), which has a known spacing of 391 Å. The beam size at the sample is approximately 100 μm by 200 μm.

Photovoltaic devices with inverted configuration were made by spin-coating a ZnO sol-gel[S6] at 4000 rpm for 60 s onto pre-cleaned, patterned ITO substrates. The photoactive layer was deposited by spin coating a chloroform solution containing the polymers and ITIC and the appropriate amount of DIO as processing additive in air. MoO_3 (10 nm) and Ag (100 nm) were deposited by vacuum evaporation at ca. 4×10^{-5} Pa as the back electrode.

The active area of the cells was 0.04 cm^2. The *J-V* characteristics were measured by a Keithley 2400 source meter unit under AM1.5G spectrum from a solar simulator (Enlitech model SS-F5-3A). Solar simulator illumination intensity was determined at 100 mW cm^{-2} using a monocrystal silicon reference cell with KG5 filter. Short circuit currents under AM1.5G conditions were estimated from the spectral response and convolution with the solar spectrum. The external quantum efficiency was measured by a Solar Cell Spectral Response Measurement System QE-R3011 (Enli Technology Co., Ltd.). The thickness of the active layers in the photovoltaic devices was measured on a Veeco Dektak XT profilometer.

Calculation of the IQE spectra was done by taking the ratio between the measured EQE and the theoretical maximum EQE predicted by a transfer matrix model.[S7] Extinction coefficients of the active materials systems were measured by using the Beer-lambert Law, with reflection and transmission of thin film samples (deposited on glass) measured by an integrating sphere. Refractive indices were simply assumed to be 2 according to reference.[S8] For modeling the theoretical maximum EQE, we used a 80 nm thick active layer for the PCBM based solar cells with a regular device structure, and a 60 nm thick active layer for the ITIC solar cells with an inverted geometry.

EL and steady-state PL measurements: EL and PL spectra were recorded by using an Andor spectrometer (Shamrock sr-303i-B, coupled to a Newton EMCCD detector). An external current/voltage source meter of Keithley 2400 was connected to the prepared photovoltaic devices comprising pure or blend films to support an external electric field for EL measurements. The pumping light sources used to measure PL is the laser with wavelength of 670 nm and an intensity of 3 mW cm^{-2}.

FTPS-EQE measurement: FTPS-EQE was carried out using a Vertex 70 from Bruker optics, equipped with a QTH lamp, quartz beamsplitter and external detector option. A low noise current amplifier (SR570) is used to amplify the photocurrent produced upon illumination of the photovoltaic devices with light modulated by the FTIR. The output voltage of the current amplifier is fed back into the external detector port of the FTIR, to be able to use the FTIR's software to collect the photocurrent spectrum.

EQE-EL measurement: The EQE-EL was recorded from a home built system with a Hamamatsu silicon photodiode 1010B. A Keithley 2400 is used for supplying voltages and recording injected current, and a Keithley 485 for measuring the emitted light intensity.

2. GPC of the polymers

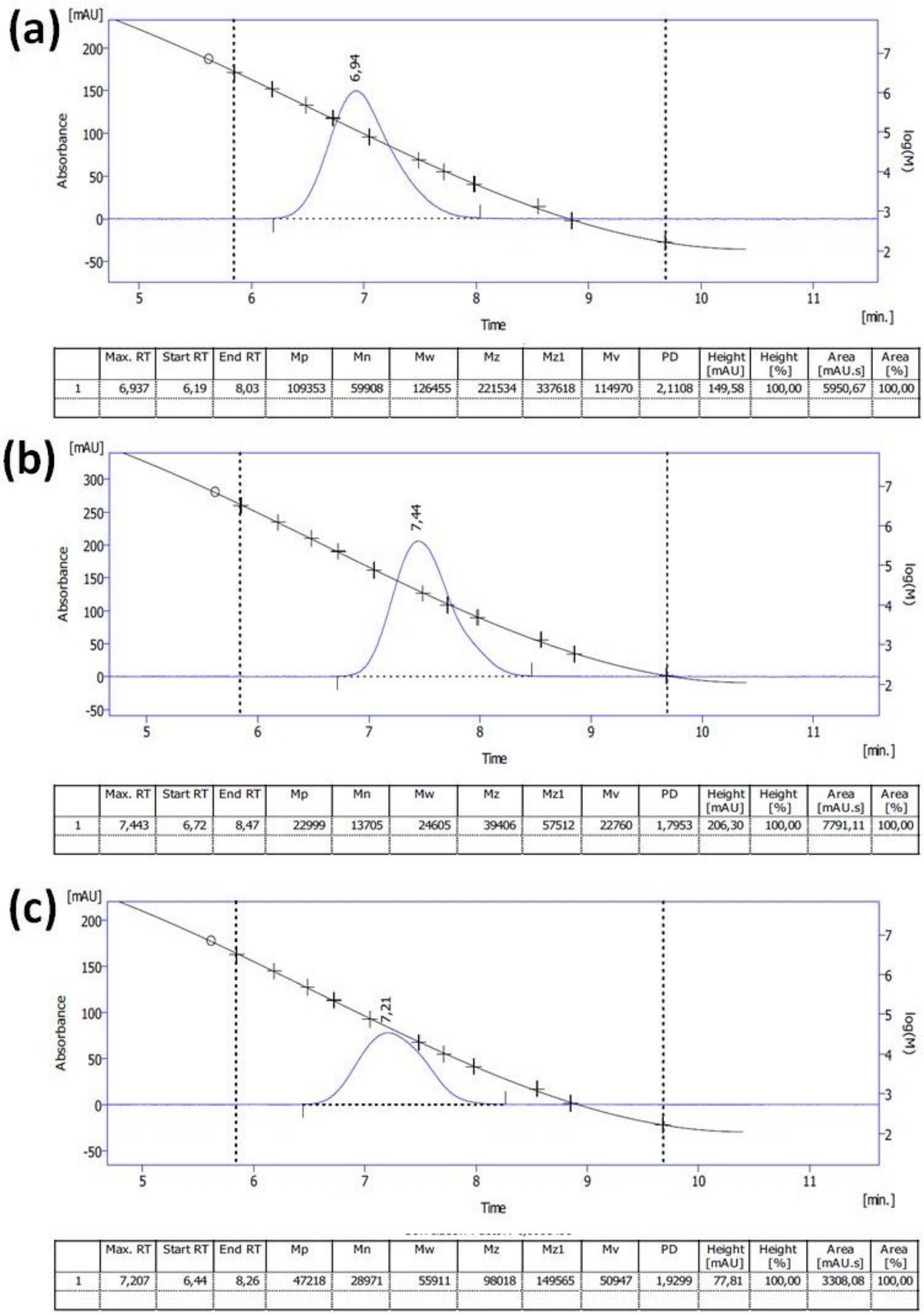

	Max. RT	Start RT	End RT	Mp	Mn	Mw	Mz	Mz1	Mv	PD	Height [mAU]	Height [%]	Area [mAU.s]	Area [%]
1	6,937	6,19	8,03	109353	59908	126455	221534	337618	114970	2,1108	149,58	100,00	5950,67	100,00

	Max. RT	Start RT	End RT	Mp	Mn	Mw	Mz	Mz1	Mv	PD	Height [mAU]	Height [%]	Area [mAU.s]	Area [%]
1	7,443	6,72	8,47	22999	13705	24605	39406	57512	22760	1,7953	206,30	100,00	7791,11	100,00

	Max. RT	Start RT	End RT	Mp	Mn	Mw	Mz	Mz1	Mv	PD	Height [mAU]	Height [%]	Area [mAU.s]	Area [%]
1	7,207	6,44	8,26	47218	28971	55911	98018	149565	50947	1,9299	77,81	100,00	3308,08	100,00

Fig. S1 GPC recorded at 140 °C with *o*-DCB as eluent for (a) PTPD3T, (b) PTPD2T and (c) PTPDBDT.

3. CV and UPS measurements

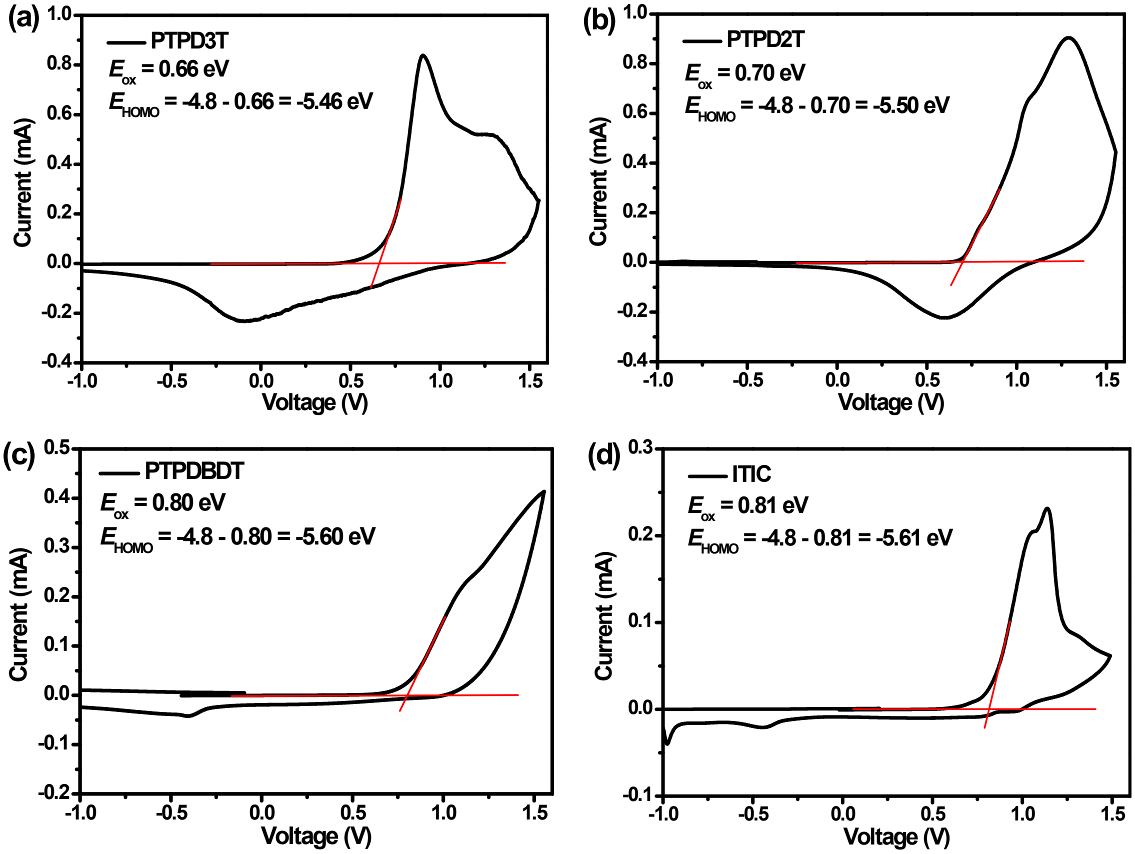

Fig. S2 Cyclic voltammogram of (a) PTPD3T, (b) PTPD2T, (c) PTPDBDT and (d) ITIC thin films. Potential vs. Fc/Fc^{+}.

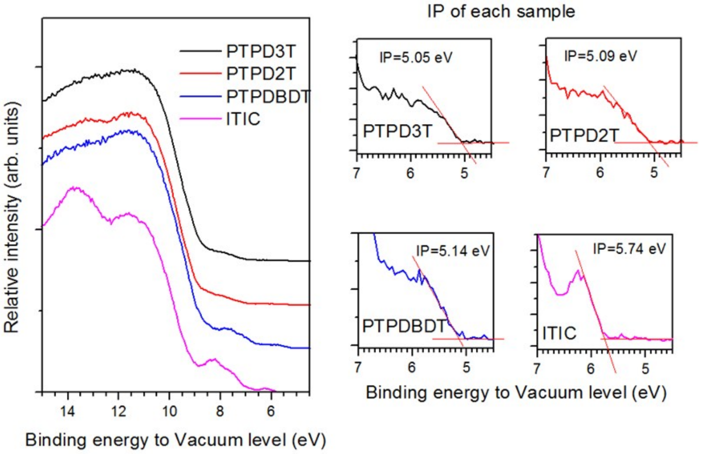

Fig. S3 UPS spectra and IP of the polymers and ITIC.

4. Solar cells of TPD polymers with ITIC as acceptor

Table S1. Characteristics of PTPD3T:ITIC inverted solar cells.

Ratio	solvent	Thickness [nm]	J_{sc}[a] [mA cm^{-2}]	V_{oc} [V]	FF	PCE [%]
1:1	$CHCl_3$	90	12.6	0.92	0.53	6.2
1:1	$CHCl_3$	110	13.4	0.91	0.59	7.2
1:1	$CHCl_3$	150	13.3	0.91	0.62	7.5
1:1	$CHCl_3$/DIO (0.2%)	65	13.3	0.91	0.65	7.9
1:1	$CHCl_3$/DIO (0.2%)	70	13.5	0.91	0.68	8.4
1:1	$CHCl_3$/DIO (0.2%)	80	13.5	0.91	0.67	8.3
1:1	$CHCl_3$/DIO (0.2%)	100	13.4	0.91	0.66	8.0
1:1	$CHCl_3$/DIO (0.5%)	80	12.8	0.93	0.65	7.7
2:1	$CHCl_3$/DIO (0.2%)	80	12.5	0.93	0.61	7.1
1:2	$CHCl_3$/DIO (0.2%)	80	13.2	0.90	0.64	7.6

[a] J_{sc} was calculated by integrating the EQE spectrum with the AM1.5G spectrum.

Table S2. Characteristics of PTPD2T:ITIC inverted solar cells.

Ratio	solvent	Thickness [nm]	J_{sc}[a] [mA cm^{-2}]	V_{oc} [V]	FF	PCE [%]
1:1	$CHCl_3$	65	11.1	0.94	0.58	6.1
1:1	$CHCl_3$/DIO (0.2%)	50	11.9	0.96	0.58	6.7
1:1	$CHCl_3$/DIO (0.2%)	60	12.3	0.96	0.60	7.0
1:1	$CHCl_3$/DIO (0.2%)	70	12.5	0.95	0.58	6.9
1:1	$CHCl_3$/DIO (0.2%)	80	11.8	0.95	0.57	6.5
1:1	$CHCl_3$/DIO (0.5%)	65	10.9	0.97	0.58	6.2
2:1	$CHCl_3$/DIO (0.2%)	70	11.0	0.96	0.53	5.6
1:2	$CHCl_3$/DIO (0.2%)	70	12.0	0.95	0.52	5.9

[a] J_{sc} was calculated by integrating the EQE spectrum with the AM1.5G spectrum.

Table S3. Characteristics of PTPDBDT:ITIC inverted solar cells.

Ratio	solvent	Thickness [nm]	J_{sc}[a] [mA cm^{-2}]	V_{oc} [V]	FF	PCE [%]

1:1	$CHCl_3$	80	6.0	1.05	0.46	2.9
1:1	$CHCl_3$/DIO (0.2%)	70	8.1	1.04	0.56	4.7
1:1	$CHCl_3$/DIO (0.2%)	85	8.5	1.05	0.60	5.4
1:1	$CHCl_3$/DIO (0.2%)	105	8.8	1.05	0.59	5.4
1:1	$CHCl_3$/DIO (0.5%)	75	8.7	1.03	0.61	5.4
2:1	$CHCl_3$/DIO (0.2%)	60	8.2	1.05	0.53	4.6
1:2	$CHCl_3$/DIO (0.2%)	75	5.4	1.03	0.49	2.7

[a]J_{sc} was calculated by integrating the EQE spectrum with the AM1.5G spectrum.

Table S4. Photovoltaic performances of 8 devices based on PTPD3T:ITIC cells fabricated from $CHCl_3$/DIO (0.2%) without thermal annealing.

No.	J_{sc} [mA cm^{-2}]	V_{oc} [V]	FF	PCE [%]
1	13.36	0.91	0.66	8.0
2	13.52	0.91	0.68	8.4
3	13.53	0.91	0.67	8.3
4	13.30	0.91	0.66	7.9
5	13.61	0.92	0.67	8.3
6	13.75	0.92	0.63	8.0
7	13.60	0.90	0.65	8.0
8	13.52	0.91	0.68	8.3
average	13.52±0.13	0.91±0.006	0.66±0.016	8.2±0.18

Table S5. Photovoltaic performances of 8 devices based on PTPD2T:ITIC cells fabricated from $CHCl_3$/DIO (0.2%) without thermal annealing.

No.	J_{sc} [mA cm^{-2}]	V_{oc} [V]	FF	PCE [%]
1	11.82	0.95	0.57	6.5
2	12.81	0.95	0.58	7.0
3	12.85	0.96	0.53	6.6
4	12.52	0.95	0.58	6.9
5	12.31	0.96	0.60	7.0
6	11.91	0.96	0.58	6.7

7	11.75	0.95	0.60	6.7
8	11.60	0.96	0.58	6.5
average	12.20±0.46	0.96±0.005	0.58±0.02	6.7±0.19

Table S6. Photovoltaic performances of 8 devices based on PTPDBDT:ITIC cells fabricated from $CHCl_3$/DIO (0.2%) without thermal annealing.

No.	J_{sc} [mA cm^{-2}]	V_{oc} [V]	FF	PCE [%]
1	8.50	1.05	0.60	5.4
2	8.84	1.05	0.59	5.4
3	8.24	1.04	0.57	4.9
4	8.08	1.04	0.56	4.7
5	8.13	1.05	0.55	4.7
6	8.20	1.05	0.53	4.6
7	8.73	1.04	0.57	5.2
8	8.30	1.07	0.52	4.6
average	8.38±0.26	1.05±0.009	0.56±0.026	4.9±0.32

5. EQE_{EL} of the optimized solar cells

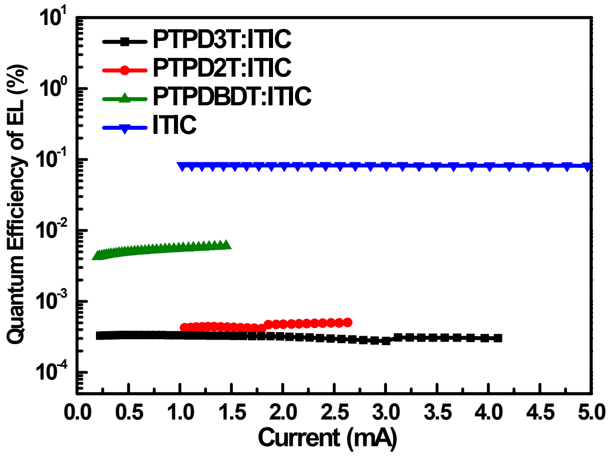

Fig. S4 EQE_{EL} of the optimized cells

6. References

(S1) Zhou, N.; Guo, X.; Ortiz, R. P.; Harschneck, T.; Manley, E. F.; Lou, S. J.; Hartnett, P. E.;

Yu, X.; Horwitz, N. E.; Burrezo, P. M.; Aldrich, T. J.; López Navarrete, J. T.; Wasielewski, M. R.; Chen, L. X.; Chang, R. P. H.; Facchetti, A.; Marks, T. J. *J. Am. Chem. Soc.* **2015**, *137*, 12565-12579.

(S2) Yuan, M.-C.; Chiu, M.-Y.; Liu, S.-P.; Chen, C.-M.; Wei, K.-H. *Macromolecules* **2010**, *43*, 6936-6938.

(S3) Yuan, J.; Zhai, Z.; Dong, H.; Li, J.; Jiang, Z.; Li, Y.; Ma, W. *Adv. Funct. Mater.* **2013**, *23*, 885-892.

(S4) Alexander, H.; Wim, B.; James, G.; Eric, S.; Eliot, G.; Rick, K.; Alastair, M.; Matthew, C.; Bruce, R.; Howard, P. *J. Phys. Conf. Ser.* **2010**, *247*, 012007.

(S5) Gann, E.; Young, A. T.; Collins, B. A.; Yan, H.; Nasiatka, J.; Padmore, H. A.; Ade, H.; Hexemer, A.; Wang, C. Soft x-ray Scattering Facility at the Advanced Light Source with Real-Time Data Processing and Analysis. *Rew. Sci. Instru.* **2012**, *83*, 045110.

(S6) Sun, Y.; Seo, J. H.; Takacs, C. J.; Seifter, J.; Heeger, A. J. *Adv. Mater.* **2011**, *23*, 1679-1683.

(S7) Pettersson, L. A. A.; Roman, L. S.; Inganäs, O. *J. Appl. Phys.* **1999**, *86*, 487-496.

(S8) Burkhard, G. F.; Hoke, E. T.; McGehee, M. D. *Adv. Mater.* **2010**, *22*, 3293-3297.